Published OnlineFirst May 29, 2015; DOI: 10.1158/2326-6066.CIR-15-0014

Priority Brief

Cancer Immunology Research

STAT3 in CD8$^+$ T Cells Inhibits Their Tumor Accumulation by Downregulating CXCR3/CXCL10 Axis

Chanyu Yue, Shudan Shen, Jiehui Deng, Saul J. Priceman, Wenzhao Li, Austin Huang, and Hua Yu

Abstract

One of the obstacles for cancer immunotherapy is the inefficiency of CD8$^+$ T-cell recruitment to tumors. STAT3 has been shown to suppress CD8$^+$ T-cell antitumor functions in various cancer models, in part by restricting accumulation of CD8$^+$ T cells. However, the underlying molecular mechanism by which STAT3 in CD8$^+$ T cells inhibits their accumulation in tumors remains to be defined. Here, we show that STAT3 signaling in CD8$^+$ T cells inhibits chemokine CXCL10 production by tumor-associated myeloid cells by reducing IFNγ expression by T cells. We further demonstrate that ablating STAT3 in T cells allows expression of CXCR3, the receptor of CXCL10, on CD8$^+$ T cells, resulting in efficient accumulation of CD8$^+$ T cells at tumor sites. Blocking IFNγ or CXCR3 impairs the accumulation of STAT3-deficient CD8$^+$ T cells in tumor and their antitumor effects. Together, our study reveals a negative regulation by STAT3 signaling in T cells on cross-talk between myeloid cells and T cells through IFNγ/CXCR3/CXCL10, which is important for CD8$^+$ T cells homing to tumors. Our results thus provide new insights applicable to cancer immunotherapy and adoptive T-cell strategies. *Cancer Immunol Res; 3(8); 864–70. ©2015 AACR.*

Introduction

A long-standing problem in tumor immunology that poses a serious challenge for cancer immunotherapy is why tumor-killing CD8$^+$ T cells do not efficiently infiltrate tumors (1, 2). In stark contrast, CD4$^+$ T cells, especially regulatory T cells, which induce immunosuppression and promote tumor growth and metastasis, accumulate in tumors (3, 4). Extensive studies from our laboratory and others show that STAT3, a Signal Transducer and Activator of Transcription family protein critical for tumor-cell survival and invasion, mediates the cross-talk between tumor cells and various immune cells, causing tumor immunosuppression (3, 5–8). Our published results suggest that STAT3 activity within regulatory CD4$^+$ T cells is critical for their tumor accumulation (3, 9). By contrast, STAT3 intrinsic to CD8$^+$ T cells inhibits their tumor infiltration (7). These findings suggest that tumor recruitment of CD4$^+$ and CD8$^+$ T cells utilizes distinct signaling pathways/factors, resulting in opposing biologic functions that ultimately enhance tumor progression.

We recently demonstrated that signaling of sphingosine-1-phosphate (S1P) and its receptor, S1PR1, which is critical for persistent STAT3 activation in tumor cells and tumor-associated immune cells (10), is essential for CD4$^+$ T regulatory cell mobilization to tumor sites, thereby indirectly affecting accumulation of tumor-associated CD8$^+$ T cells (9). However, little is understood about the detailed intrinsic molecular mechanisms by which CD8$^+$ T cells home to tumor sites. Several chemokines have been shown to be important for inducing CD8$^+$ T-cell recruitment to tumor sites (11–13). CXCR3, the receptor for its chemokine ligand CXCL9/10, has been shown to facilitate CD8$^+$ T-cell recruitment in inflammatory and infectious diseases (14, 15). CXCR3 is also known to be important for T-cell trafficking and effector T-cell generation (16). Consistent with this notion, CD8$^+$ T-cell accumulation in the intestinal environment after acute injury depends on CXCR3 (17). At the same time, both CXCL10 and CXCR3 have been shown to be favorable prognostic markers and correlate with enhanced survival rate in both renal cell carcinoma and melanoma (18, 19). On the other hand, CXCR3 is found to be expressed and functional in almost all cells and upregulated in many primary and metastatic tumors, and considered to be crucial for cancer cell migration (20). We address in the current study whether and how STAT3 regulates CD8$^+$ T-cell recruitment to tumor via IFNγ–CXCL10–CXCR3 signaling.

Materials and Methods

Mice

Stat3$^{loxp/loxp}$ (*Stat3*$^{+/+}$) mice were kindly provided by Drs. Shizuo Akira and Kiyoshi Takeda (Osaka University, Japan) and crossed with *CD4-Cre* mice (Taconic) to generate *CD4-Cre/Stat3*$^{loxp/loxp}$ mice with *Stat3* deletion in T cells (*Stat3*$^{-/-}$) as previously described (7, 9). *Rag1*$^{-/-}$ mice were purchased from the Jackson Laboratory. Mouse care and experimental procedures were performed in accordance with established institutional guidance and approved protocols from the Institutional Animal

Department of Cancer Immunotherapeutics and Tumor Immunology, City of Hope Comprehensive Cancer Center, Duarte, California.

Note: Supplementary data for this article are available at Cancer Immunology Research Online (http://cancerimmunolres.aacrjournals.org/).

C. Yue and S. Shen contributed equally to this article.

Corresponding Author: Hua Yu, City of Hope Comprehensive Cancer Center, 1500 East Duarte Road, Duarte CA 91010. Phone: 626-256-4673, ext. 63365; Fax: 626-256-8708; E-mail: hyu@coh.org

doi: 10.1158/2326-6066.CIR-15-0014

Care and Use Committee at the Beckman Research Institute of City of Hope National Medical Center.

In vivo tumor establishment and T-cell–adoptive transfer

The B16 mouse melanoma and 3LL mouse Lewis Lung carcinoma cell lines were obtained from the American Type Culture Collection and maintained in RPMI 1640 media (B16) or DMEM media (3LL) containing 10% FBS, respectively. For tumor challenge, B16 or 3LL cells were implanted subcutaneously into 8- to 10-week-old *Stat3*$^{+/+}$ or *Stat3*$^{-/-}$ mice (5×10^5/mouse). Tumors, spleens, or tumor-draining lymph nodes (TDLN) were harvested 10 to 14 days after tumor-cell injection for further analysis. For T-cell adoptive transfer, mice received intravenous injection of 8×10^6 CD8$^+$ T cells 1 day prior to tumor challenge (3×10^5 B16 cells). CD8$^+$ T cells were isolated from spleens of 8- to 10-week-old *Stat3*$^{+/+}$ or *Stat3*$^{-/-}$ mice by magnetic bead enrichment using CD8$^+$ T-cell negative selection EasySep kits (StemCell Technologies). Subcutaneous injection near the tumor sites of PBS (vehicle control), anti-IFNγ peptide (JPT Peptide, 200 μg/mouse), and CXCR3 antagonist SCH 546738 (MedChem Express; 600 μg/mouse) was started on day 6 after tumor injection and was performed daily for up to 1 week.

In vitro T-cell migration assay

Spleens and lymph nodes were gently dissociated under 70-μm nylon mesh for single-cell isolation. Cell pellets were resuspended in red blood cell lysing buffer (Sigma-Aldrich) to remove red blood cells, and single-cell suspensions were filtered, washed, and resuspended in FACS Wash Buffer (2% FBS in Hank's Balanced Salt Solution without Ca^{2+}, Mg^{2+}, and phenol red). Total splenocytes harvested from tumor-bearing mice were stained with APC-CD3 and PE-CD8 antibodies. Cells were then washed three times and resuspended in migration buffer to a final concentration of 1×10^7 cells/mL. Migration assays were carried out by seeding T cells in the upper chamber of 96-well Transwell plates with 5.0-μm pore size polycarbonate membrane (Corning). Cells (50 μL) were added into each top well and allowed to migrate at 37°C for 2 to 3 hours. The lower chambers were filled with 200 μL of migration buffer (RPMI-1640 medium with 0.1% fatty acid–free BSA and 10 mmol/L HEPES) with or without murine CXCL10 (PeproTech) as chemoattractant for migration. In some experiments, cells were pretreated with small GTPase inhibitors, CT04 (Rho A family inhibitor; Cytoskeleton), ROCKi (Rho Kinase inhibitor; Millipore), ML141 (Cdc42 inhibitor; Tocris Bioscience), and NSC23766 (Rac1 inhibitor; Santa Cruz Biotechnology), or CXCR3 antagonist SCH 546738, at indicated times and doses. Migrated cells in the bottom chambers were enumerated by flow cytometry at a fixed flow rate for 1 minute on an Accuri C6 flow cytometer. Data were presented in fold changes, where the number of cells from the control group (Ctrl) was set at one. Triplicates were performed for each condition.

Flow cytometry for surface and intracellular staining

Single-cell suspensions from tumors (prepared as previously described; ref. 9) and TDLNs were stained with FITC-CD3 and PE-CD8 antibodies, then fixed and permeabilized using the Foxp3/Transcription Factor Fixation/Permeabilization Kit (eBioscience) according to the manufacturer's protocol. Following two washes, cells were stained for 30 minutes on ice with APC-IFNγ. Cells were washed twice and resuspended in FACS buffer before flow cytometry analysis. Data were collected using an Accuri C6 flow cytometer and analyzed with FlowJo software (TreeStar).

Real-time quantitative PCR

CD8$^+$ T cells or CD11b$^+$ myeloid cells were enriched from tumor-cell mixtures, TDLNs, or spleens from B16 tumor–bearing *Stat3*$^{+/+}$ or *Stat3*$^{-/-}$ mice, as described above. In some experiments, CD11b$^+$F4/80$^+$ myeloid cells were sorted by FACSAria SORP cell sorter (BD Bioscience) from tumor-cell mixtures. Total RNA was extracted using RNAqueous Micro kit column purification (Ambion). cDNA was produced from RNA using a cDNA synthesis kit (Bio-Rad). Quantitative RT-PCR was performed using SYBR Green Supermix (Bio-Rad) and quantified using Chromo4 real-time detector (Bio-Rad). RT-PCR primers were purchased from SA Biosciences. Each primer set was validated using a standard curve across the dynamic range of interest with a single melting peak.

Western blotting and ELISA

For Western blotting, CD8$^+$ T cells were negatively enriched as described above. Cells were lysed in 1% Nonidet P-40 lysis buffer containing protease inhibitor cocktail (Sigma-Aldrich) and 1 mmol/L sodium orthovanadate (Sigma-Aldrich). Protein lysates (20 μg) were subjected to SDS-PAGE, probed with indicated antibodies, and detected using an enhanced chemiluminescence substrate (Pierce). Monoclonal anti–β-actin antibody was purchased from Sigma-Aldrich. Polyclonal antibody against CXCR3 was purchased from Abcam. For determination of CXCL10 levels, 1×10^6 B16 total tumor cells or B16 tumor–infiltrating CD11b$^+$ myeloid cells, isolated as mentioned above, were incubated with 1 mL of serum-free medium, and supernatants were collected from a 24-hour cell culture. Tumor-cell supernatants were subjected to murine IP-10 ELISA and analyzed according to the manufacturer's instructions (Peprotech).

Immunostaining

Formalin-fixed paraffin-embedded sections were deparaffinized, followed by Ag retrieval with high pH Ag retrieval solution (Vector Labs), and stained with antibody against mouse CD8 (Biolegend), followed by incubation with Alexa555-labeled goat anti-mouse IgG with Hoechest 33342. Quantification was performed by acquiring images of three random fields per sample under ×40 magnifications with a Nikon Eclipse TE2000-U microscope, followed by analysis with Image-Pro Plus (Media Cybernetics).

Statistical analysis

Data are presented as mean ± SEM. Statistical comparisons between groups were performed using the unpaired Student *t* test to calculate two-tailed *P* value. *, $P < 0.05$; **, $P < 0.01$; ***, $P < 0.001$; ns, not significant.

Results and Discussion

STAT3 affects CD8$^+$ T-cell migration to tumors by inhibiting tumor-associated myeloid cell chemokine expression

We first assessed whether *Stat3* in T cells would affect chemokine expression by tumor-associated myeloid cells. B16 murine melanoma cells were subcutaneously implanted in wild-type (*Stat3*$^{loxp/loxp}$, referred to as *Stat3*$^{+/+}$) and T-cell *Stat3*-deficient (*CD4-Cre*/*Stat3*$^{loxp/loxp}$, referred to as *Stat3*$^{-/-}$)

Published OnlineFirst May 29, 2015; DOI: 10.1158/2326-6066.CIR-15-0014

mice. The CD4-driven Cre recombinase is able to delete the loxp-flanked *Stat3* during the $CD4^+CD8^+$ double-positive stage of early T-cell development. CXCL9, CXCL10, and CXCL11 provide cues for different types of cells, including T cells, during infection and inflammation (17, 21, 22), and thus we assessed the effects of Stat3 ablation in T cells on their expression by tumor-associated myeloid cells. Tumors were harvested 10 to 14 days after implantation, and different cell populations, including tumor cells and $CD11b^+$ myeloid cells, were enriched from the tumor-cell mixtures. Real-time PCR analysis of different chemokines revealed that expression of *Cxcl9*, *Cxcl10*, and, to a lesser degree, *Cxcl11*, was significantly upregulated within tumor-associated myeloid cells by the loss of *Stat3* in T cells (Fig. 1A, left three plots). The enhanced production of CXCL10 by myeloid cells due to *Stat3* ablation in T cells was further confirmed by using ELISA in both the B16 melanoma and 3LL (Lewis Lung Carcinoma) mouse tumor models (Fig. 1A, right two plots). However, the mRNA expression in *Cxcl9*, *Cxcl10*, and *Cxcl11* of total tumor cells was not affected by *Stat3* ablation in T cells (Supplementary Fig. S1A). In addition, CXCL10 secretion by total tumor cells remained unchanged (Supplementary Fig. S1B). Moreover, the levels of CXCL10 secreted by total tumor cells were at basal (~0.2 ng/mL, Supplementary Fig. S1B), compared with CXCL10 levels secreted by myeloid cells (~1–3 ng/mL, Fig. 1A). This indicates that loss of *Stat3* in T cells did not affect production of chemokines by tumor cells, which are the main population of tumors, but rather had a dramatic and selective effect on tumor-associated myeloid cell production of these chemokines. To further identify subpopulations of myeloid cells, we sorted $CD11b^+$ tumor-infiltrating myeloid cells and found that nearly 80% of them were $F4/80^+$ macrophages (Supplementary Fig. S2A). As expected, macrophages from $Stat3^{-/-}$ mice showed significantly elevated levels of *Cxcl10* mRNA (Supplementary Fig. S2B).

Because CXCL9, CXCL10, and CXCL11 are known to be regulated by IFNγ, we determined the effects of *Stat3* ablation on the percentage of $IFN\gamma^+$ $CD8^+$ T cells in tumors. Real-time PCR analysis showed significantly increased expression of IFNγ in *Stat3* knockout $CD8^+$ T cells from TDLNs (Fig. 1B, left), which was confirmed by flow cytometry analysis (Fig. 1B, right, 6.62% vs. 16.1% in TDLNs). Flow cytometry analysis also showed that $IFN\gamma^+$ cells are increased in tumor-infiltrating $CD8^+$ T cells upon *Stat3* deletion in T cells (Fig. 1B, right, 4.85% vs. 14.5%). To address whether CXCL10 can attract $CD8^+$ T-cell migration, we performed an *in vitro* migration assay using $CD8^+$ T cells from spleens of tumor-bearing mice and demonstrated that indeed CXCL10 stimulates $CD8^+$ T-cell

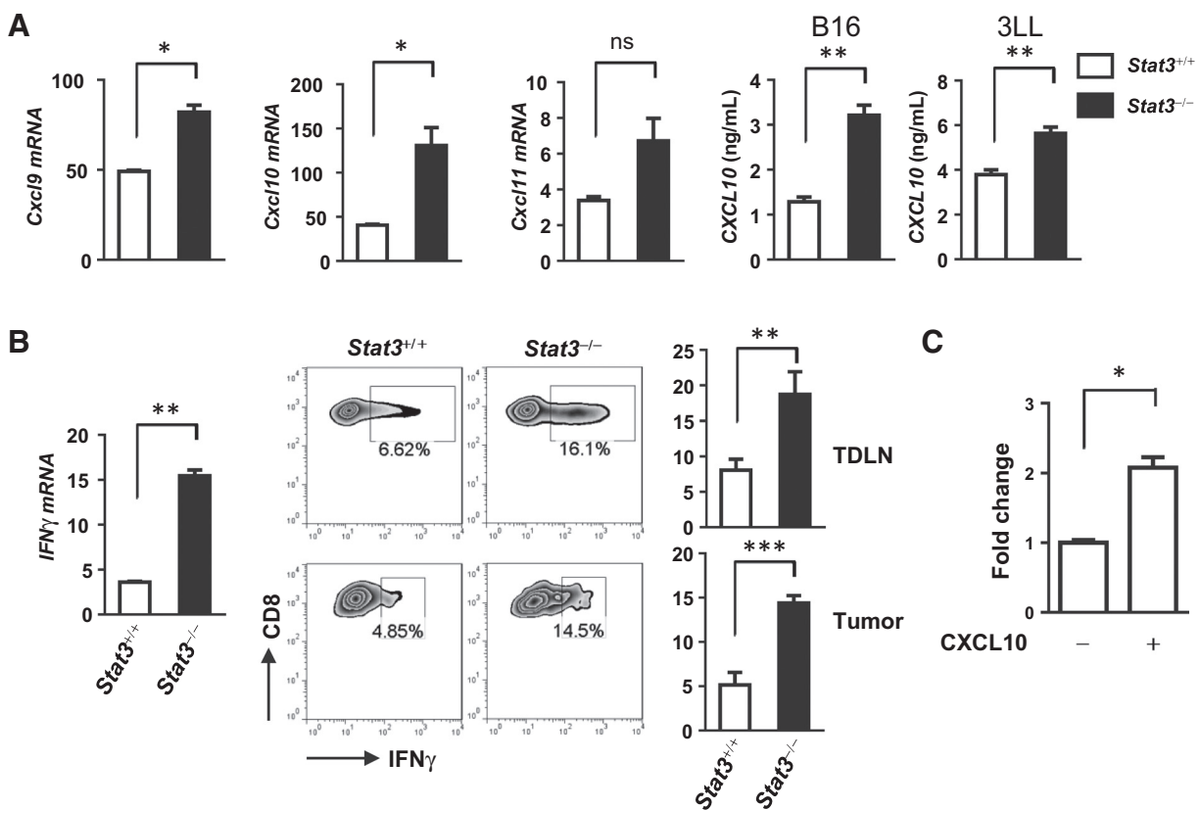

Figure 1.
STAT3 in T cells drives tumor-associated myeloid cell chemokine expression. A, left three plots, real-time PCR analysis of *Cxcl9*, *Cxcl10*, and *Cxcl11* mRNA levels in tumor-infiltrating $CD11b^+$ cells from B16 tumor–bearing $Stat3^{+/+}$ ($Stat3^{loxp/loxp}$) or $Stat3^{-/-}$ ($CD4\text{-}Cre/Stat3^{loxp/loxp}$) mice. Right two plots, ELISA analysis of the CXCL10 protein levels in the conditioned medium from B16- or 3LL-infiltrating $CD11b^+$ cells from $Stat3^{+/+}$ or $Stat3^{-/-}$ mice. B, left, real-time PCR analysis of IFNγ mRNA levels in $CD8^+$ T cells harvested from TDLNs of B16 tumor–bearing $Stat3^{+/+}$ or $Stat3^{-/-}$ mice. Middle and right, flow cytometry analysis of intracellular staining of IFNγ in $CD8^+$ T cells from TDLNs or B16 tumors harvested from $Stat3^{+/+}$ or $Stat3^{-/-}$ mice with representative plots and quantification. C, migration assay analysis of splenic $CD8^+$ T cells from B16 tumor–bearing $Stat3^{+/+}$ mice in the presence or absence of CXCL10 (100 ng/mL). All data shown are representative of two to four independent experiments. *, $P < 0.05$; **, $P < 0.01$; ***, $P < 0.001$. ns, not statistically significant.

Published OnlineFirst May 29, 2015; DOI: 10.1158/2326-6066.CIR-15-0014

migration (Fig. 1C). Together, these data suggest that STAT3 signaling in T cells inhibits IFNγ production by CD8$^+$ T cells, leading to decreased IFNγ-induced chemokine expression, especially CXCL10 by tumor-associated myeloid cells. This reduction in CXCL10 expression by tumor-associated myeloid cells had a negative impact on CD8$^+$ T-cell migration. Due to the elevated STAT3 activation found in most solid tumors, the reduced chemokine expression by tumor-associated myeloid cells may account for inefficient cytotoxic CD8$^+$ T-cell accumulation.

STAT3 inhibits CXCR3 expression and CXCL10-induced CD8$^+$ T-cell migration

We next analyzed expression of CXCR3, the receptor of CXCL9/10, in CD8$^+$ T cells. Compared with naïve mice, *Cxcr3* expression was suppressed in tumor-bearing mice (Fig. 2A and B). When challenged with B16 tumors, ablation of *Stat3* in T cells resulted in increased percentage of CXCR3$^+$ splenic CD8$^+$ T cells compared with that in *Stat3*$^{+/+}$ mice by flow cytometry (Fig. 2A). Consistently, the *Cxcr3* expression in splenic CD8$^+$ T cells from tumor-bearing mice was also increased as determined by real-time PCR (Fig. 2B, top). In addition, Western blotting analysis revealed a similar change in CXCR3 expression of tumor-bearing splenic CD8$^+$ T cells (Fig. 2B, bottom). Absence of STAT3 expression did not lead to changes of CXCR3 levels in B16 tumor–primed TDLNs (Supplementary Fig. S3). It has been shown that chemokine receptors, including CXCR3, are downregulated due to internalization upon ligand binding at the target organ (23). Moreover, STAT3 has been shown to regulate IFNγ production by T cells in the tumor, but whether STAT3 can modulate CXCL10-induced CD8$^+$ T-cell migration remains unknown. *In vitro* migration assay of *Stat3*$^{+/+}$ and *Stat3*$^{-/-}$ CD8$^+$ T cells from spleens of B16 tumor–bearing mice showed enhanced migration of CD8$^+$ T cells toward CXCL10 in a dose-dependent manner in the absence of *Stat3* (Fig. 2C and D). Blocking of CXCR3 by pretreating CD8$^+$ T cells with CXCR3 antagonist SCH 546738 for 15 minutes significantly restricted CD8$^+$ T-cell migration toward CXCL10 (Fig. 2C). These results suggest that CXCR3-mediated CD8$^+$ T-cell migration is suppressed in tumors, and STAT3 negatively regulates CXCL10-induced CD8$^+$ T-cell migration by inhibiting CXCR3 expression.

IFNγ/CXCL10/CXCR3 signaling induced by *Stat3* ablation promotes tumor infiltration of CD8$^+$ T cells

To assess whether IFNγ-induced CXCL10/CXCR3 signaling due to *Stat3* ablation in T cells leads to CD8$^+$ T-cell tumor accumulation, *Stat3*$^{+/+}$ and *Stat3*$^{-/-}$ CD8$^+$ T cells were introduced into *Rag1*$^{-/-}$ mice, followed by inoculation of B16 tumor cells. When the tumors were palpable, *Rag1*$^{-/-}$ mice receiving the *Stat3*$^{+/+}$ and *Stat3*$^{-/-}$ CD8$^+$ T cells were treated with PBS (vehicle control),

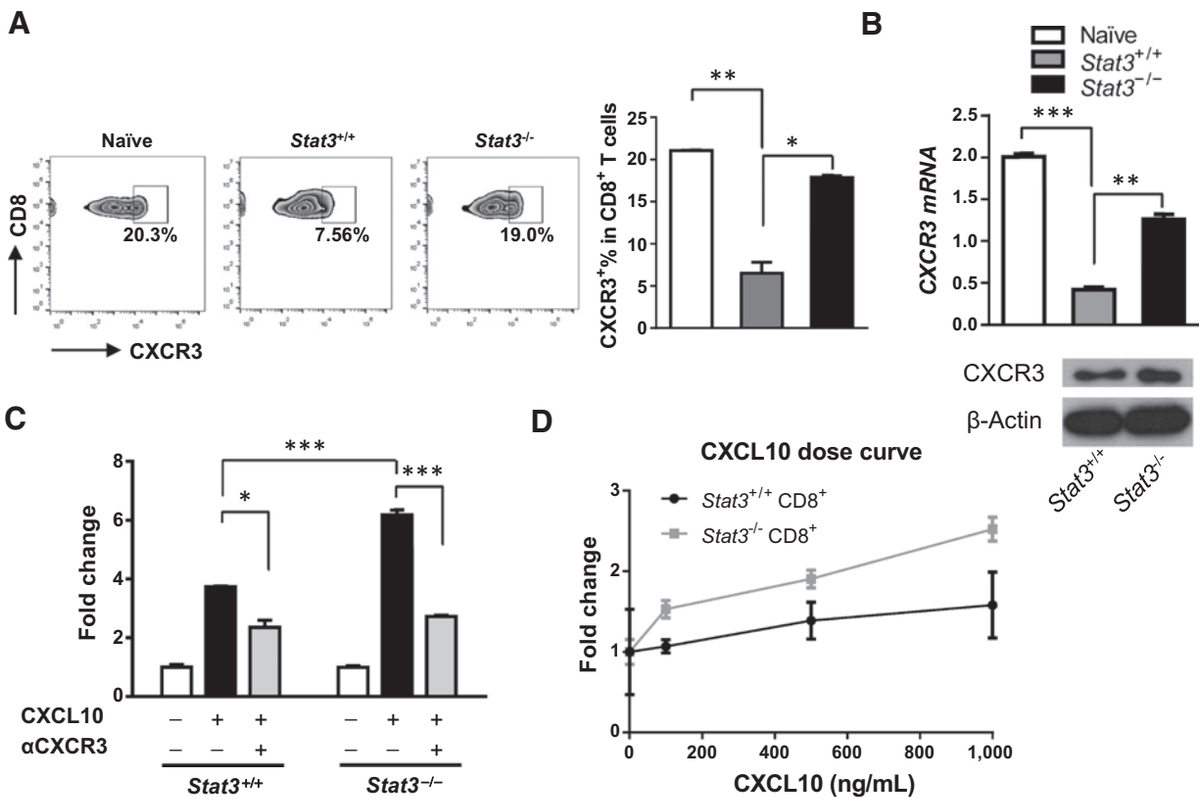

Figure 2.
CXCL10-induced CD8$^+$ T-cell migration is inhibited by STAT3-mediated suppression of CXCR3. A, left, representative flow plot and (right) quantification analysis of CXCR3 in splenic CD8$^+$ T cells from naïve or B16 tumor–bearing *Stat3*$^{+/+}$ or *Stat3*$^{-/-}$ mice. B, real-time PCR and Western blot analysis of CXCR3 in splenic CD8$^+$ T cells from naïve or B16 tumor–bearing *Stat3*$^{+/+}$ or *Stat3*$^{-/-}$ mice. C, *in vitro* migration of splenic CD8$^+$ T cells from B16 tumor–bearing *Stat3*$^{+/+}$ or *Stat3*$^{-/-}$ mice toward CXCL10 (100 ng/mL), pretreated with CXCR3 antagonist SCH 546738 (20 nmol/L) for 15 minutes. D, *in vitro* migration of splenic CD8$^+$ T cells from B16 tumor–bearing *Stat3*$^{+/+}$ or *Stat3*$^{-/-}$ mice toward CXCL10 at indicated doses. Ctrl (Control), migration media without chemoattractant. All data shown are representative of two to four independent experiments. *, $P < 0.05$; **, $P < 0.01$; ***, $P < 0.001$.

Published OnlineFirst May 29, 2015; DOI: 10.1158/2326-6066.CIR-15-0014

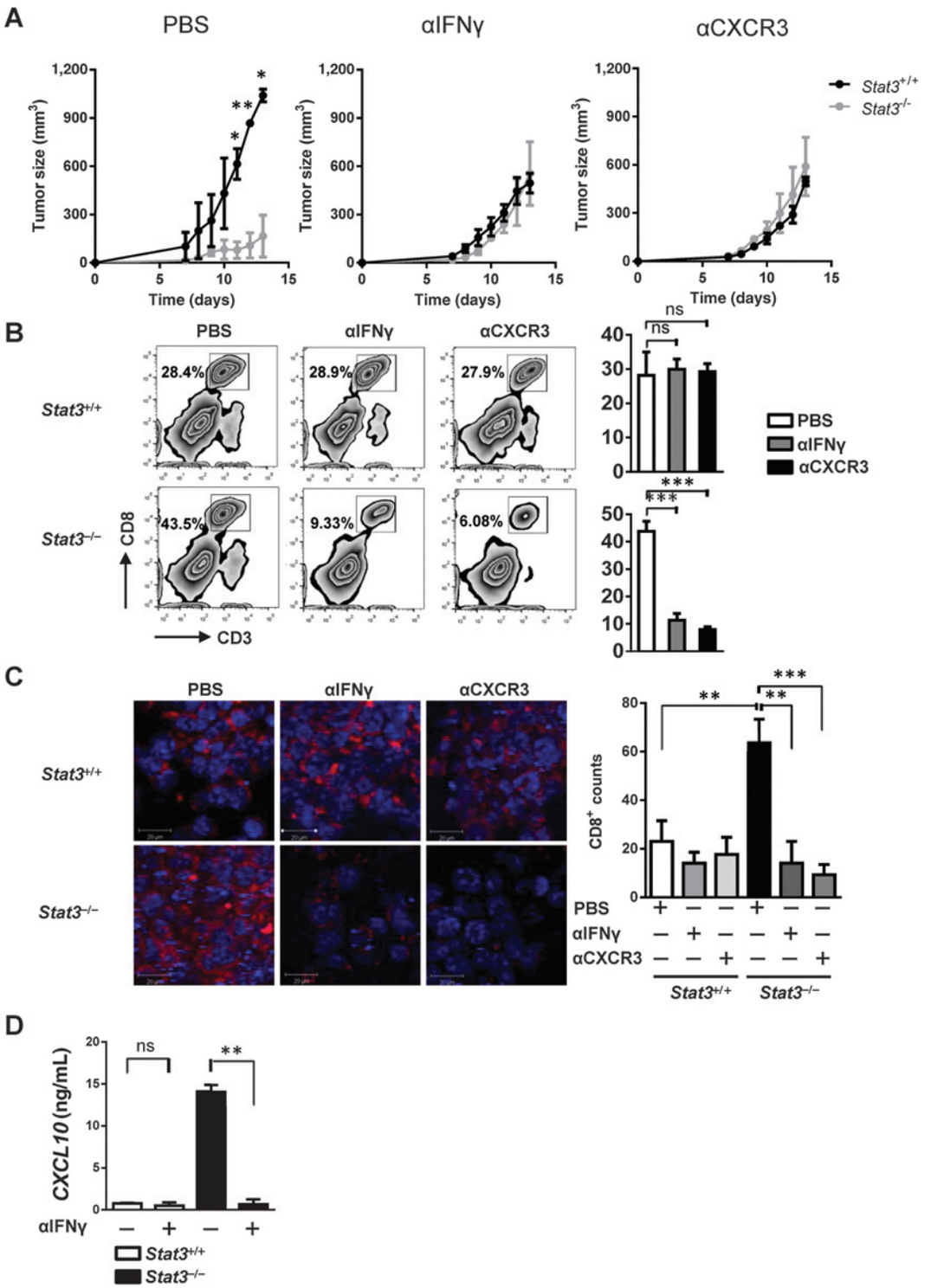

Figure 3.

Blocking IFNγ or CXCR3 abrogates STAT3-deficient $CD8^+$ T-cell tumor accumulation and associated tumor growth inhibition. A, tumor growth in *Rag1*$^{-/-}$ mice adoptively transferred with splenic $CD8^+$ T cells from *Stat3*$^{+/+}$ or *Stat3*$^{-/-}$ mice 1 day prior to B16 tumor injection, and treated 6 days later with PBS (vehicle control), anti-IFNγ peptide, or CXCR3 antagonist until day 13. B, left, representative flow plot of tumor-infiltrating T cells, gated on $CD3^+$ $CD8^+$ T cells in indicated groups. Right, quantification of $CD3^+$ $CD8^+$ T-cell percentages. C, left, immunofluorescence staining of B16 tumor–infiltrating $CD8^+$ T cells in indicated groups (CD8, red; Hoechst, blue). Right, $CD8^+$ T-cell counts from an average of 3 random sites per tumor in indicated groups. D, ELISA of CXCL10 protein levels in conditioned media from B16 tumor–infiltrating $CD11b^+$ cells from *Stat3*$^{+/+}$ or *Stat3*$^{-/-}$ mice treated with PBS (vehicle control) or with anti-IFNγ peptide. All data shown are representative of two to four independent experiments. *, $P < 0.05$; **, $P < 0.01$; ***, $P < 0.001$. ns, not statistically significant.

anti-IFNγ peptide, or CXCR3 antagonist, as indicated (Fig. 3A). As reported before, adoptive transfer of *Stat3*$^{-/-}$ CD8$^+$ T cells promoted CD8$^+$ T-cell tumor infiltration and inhibited tumor progression (Fig. 3A and B; ref. 7). Blocking IFNγ or CXCR3 in the tumor microenvironment abrogated the restricted tumor development due to *Stat3* ablation in T cells, which was accompanied by the decreased *Stat3*$^{-/-}$ CD8$^+$ T-cell accumulation at tumor sites (Fig. 3A and B), while both treatments seemed to restrict tumor development to some extent. As expected, blockade of IFNγ showed a more pronounced reduction of IFNγ-producing CD8$^+$ T cells in the absence of *Stat3* (Supplementary Fig. S4), which correlated with the reduced *Stat3*$^{-/-}$ CD8$^+$ T-cell accumulation at tumor sites. We also performed immunofluorescence staining on B16 tumor sections, which demonstrated that blockade of IFNγ or CXCR3 led to significant decreases of *Stat3*$^{-/-}$ CD8$^+$ T-cell accumulation at tumor sites (Fig. 3C, images and counts on the right). In addition, we performed CXCL10 ELISA from supernatants of tumor-associated CD11b$^+$ myeloid cells enriched from B16 tumors. Blockade of IFNγ *in vivo* reduced *Stat3* ablation–mediated CXCL10 secretion from tumor-associated myeloid cells (Fig. 3D). Together, these results show that STAT3 in T cells inhibits IFNγ–CXCL10/CXCR3 signaling by CD8$^+$ T/myeloid cells, thereby inhibiting CD8$^+$ T-cell migration to tumors *in vivo* and promoting tumor growth.

GTPases, including RhoA, Rac1, and Cdc42, are known to critically regulate cell migration, in part by regulating the actin cytoskeleton (24). We next determined which small GTPase is responsible for CXCL10–CXCR3 signaling-mediated CD8$^+$ T-cell migration. Use of an *in vitro* migration assay with CD8$^+$ T cells demonstrated that pretreatment with either a RhoA family or a Rho kinase inhibitor blocked CXCL10-induced CD8$^+$ T-cell migration, independent of *Stat3* expression (Supplementary Fig. S5A), whereas inhibition of Cdc42 or Rac1 had no effect on CXCL10-mediated CD8$^+$ T-cell migration (Supplementary Fig. S5B). These results suggest that CXCL10-induced CD8$^+$ T-cell migration depends on Rho signaling, which is in agreement with a recent finding in which LFA-1–directed T-cell motility was shown to depend on Rho GTPase signaling (25).

In summary, as depicted in Supplementary Fig. S6, we have demonstrated that STAT3 inhibits CD8$^+$ T-cell accumulation in tumor sites through downregulating IFNγ production by CD8$^+$ T cells, leading to decreased production of IFNγ-induced chemokines, especially CXCL10, by tumor-associated myeloid cells. STAT3 also negatively regulates T-cell CXCR3 expression in the tumor microenvironment, further hampering tumor infiltration of CD8$^+$ T cells. Together, these studies shed light on targeting strategies for enhancing CD8$^+$ T-cell homing to tumors as a means to improve cancer immunotherapies and adoptive T-cell strategies.

Disclosure of Potential Conflicts of Interest

No potential conflicts of interest were disclosed.

Authors' Contributions

Conception and design: C. Yue, S. Shen, J. Deng, H. Yu
Development of methodology: C. Yue, S. Shen, S.J. Priceman, W. Li, A. Huang
Acquisition of data (provided animals, acquired and managed patients, provided facilities, etc.): C. Yue, S. Shen, W. Li
Analysis and interpretation of data (e.g., statistical analysis, biostatistics, computational analysis): C. Yue, J. Deng, S.J. Priceman
Writing, review, and/or revision of the manuscript: C. Yue, J. Deng, H. Yu
Study supervision: H. Yu

Acknowledgments

The authors thank staff members of the Flow Cytometry Core and Animal Facility Core in the Beckman Research Institute at City of Hope Comprehensive Cancer Center for excellent technical assistance.

Grant Support

The research reported in this publication was supported by the National Cancer Institute of the National Institutes of Health under grant numbers R01CA122976, U54CA163117, and R01CA146092, as well as by the National Cancer Institute of the National Institutes of Health under grant number P30CA033572. This study was also supported by Tim Nesviq Fund at City of Hope Comprehensive Cancer Center and the HEADstrong Foundation in memory of Nicholas E. Colleluori.

Received January 14, 2015; revised May 11, 2015; accepted May 20, 2015; published OnlineFirst May 29, 2015.

References

1. June CH. Adoptive T cell therapy for cancer in the clinic. J Clin Invest 2007;117:1466–76.
2. June CH. Principles of adoptive T cell cancer therapy. J Clin Invest 2007;117:1204–12.
3. Kortylewski M, Kujawski M, Wang T, Wei S, Zhang S, Pilon-Thomas S, et al. Inhibiting Stat3 signaling in the hematopoietic system elicits multicomponent antitumor immunity. Nat Med 2005;11:1314–21.
4. Zou W. Regulatory T cells, tumour immunity and immunotherapy. Nat Rev Immunol 2006;6:295–307.
5. Frank DA. STAT3 as a central mediator of neoplastic cellular transformation. Cancer Lett 2007;251:199–210.
6. Herrmann A, Kortylewski M, Kujawski M, Zhang C, Reckamp K, Armstrong B, et al. Targeting Stat3 in the myeloid compartment drastically improves the in vivo antitumor functions of adoptively transferred T cells. Cancer Res 2010;70:7455–64.
7. Kujawski M, Zhang C, Herrmann A, Reckamp K, Scuto A, Jensen M, et al. Targeting STAT3 in adoptively transferred T cells promotes their in vivo expansion and antitumor effects. Cancer Res 2010;70:9599–610.
8. Yu H, Lee H, Herrmann A, Buettner R, Jove R. Revisiting STAT3 signalling in cancer: new and unexpected biological functions. Nat Rev Cancer 2014;14:736–46.
9. Priceman SJ, Shen S, Wang L, Deng J, Yue C, Kujawski M, et al. S1PR1 is crucial for accumulation of regulatory T cells in tumors via STAT3. Cell Reports 2014;6:992–9.
10. Lee H, Deng J, Kujawski M, Yang C, Liu Y, Herrmann A, et al. STAT3-induced S1PR1 expression is crucial for persistent STAT3 activation in tumors. Nat Med 2010;16:1421–8.
11. Johrer K, Pleyer L, Olivier A, Maizner E, Zelle-Rieser C, Greil R. Tumour-immune cell interactions modulated by chemokines. Expert Opin Biol Ther 2008;8:269–90.
12. Mule JJ, Custer M, Averbook B, Yang JC, Weber JS, Goeddel DV, et al. RANTES secretion by gene-modified tumor cells results in loss of tumorigenicity in vivo: role of immune cell subpopulations. Human Gene Ther 1996;7:1545–53.
13. Peng W, Ye Y, Rabinovich BA, Liu C, Lou Y, Zhang M, et al. Transduction of tumor-specific T cells with CXCR2 chemokine receptor improves migration to tumor and antitumor immune responses. Clin Cancer Res 2010;16:5458–68.
14. Bromley SK, Mempel TR, Luster AD. Orchestrating the orchestrators: chemokines in control of T cell traffic. Nat Immunol 2008;9:970–80.
15. Sung JH, Zhang H, Moseman EA, Alvarez D, Iannacone M, Henrickson SE, et al. Chemokine guidance of central memory T cells is

Published OnlineFirst May 29, 2015; DOI: 10.1158/2326-6066.CIR-15-0014

critical for antiviral recall responses in lymph nodes. Cell 2012;150: 1249–63.
16. Groom JR, Luster AD. CXCR3 ligands: redundant, collaborative and antagonistic functions. Immunol Cell Biol 2011;89: 207–15.
17. Wu X, Lahiri A, Haines GK 3rd, Flavell RA, Abraham C. NOD2 regulates CXCR3-dependent CD8+ T cell accumulation in intestinal tissues with acute injury. J Immunol 2014;192:3409–18.
18. Kondo T, Ito F, Nakazawa H, Horita S, Osaka Y, Toma H. High expression of chemokine gene as a favorable prognostic factor in renal cell carcinoma. J Urol 2004;171:2171–5.
19. Mullins IM, Slingluff CL, Lee JK, Garbee CF, Shu J, Anderson SG, et al. CXC chemokine receptor 3 expression by activated CD8+ T cells is associated with survival in melanoma patients with stage III disease. Cancer Res 2004;64:7697–701.
20. Ma B, Khazali A, Wells A. CXCR3 in carcinoma progression. Histol Histopathol 2015;11594.
21. Peng W, Liu C, Xu C, Lou Y, Chen J, Yang Y, et al. PD-1 blockade enhances T-cell migration to tumors by elevating IFN-gamma inducible chemokines. Cancer Res 2012;72:5209–18.
22. Shin SY, Nam JS, Lim Y, Lee YH. TNFalpha-exposed bone marrow-derived mesenchymal stem cells promote locomotion of MDA-MB-231 breast cancer cells through transcriptional activation of CXCR3 ligand chemokines. J Biol Chem 2010;285:30731–40.
23. Sharma RK, Chheda Z, Jala VR, Haribabu B. Expression of leukotriene B (4) receptor-1 on CD8(+) T cells is required for their migration into tumors to elicit effective antitumor immunity. J Immunol 2013; 191:3462–70.
24. Scheele JS, Marks RE, Boss GR. Signaling by small GTPases in the immune system. Immunol Rev 2007;218:92–101.
25. Ramsay AG, Evans R, Kiaii S, Svensson L, Hogg N, Gribben JG. Chronic lymphocytic leukemia cells induce defective LFA-1-directed T-cell motility by altering Rho GTPase signaling that is reversible with lenalidomide. Blood 2013;121:2704–14.

Published OnlineFirst May 29, 2015; DOI: 10.1158/2326-6066.CIR-15-0014

Cancer Immunology Research

STAT3 in CD8$^+$ T Cells Inhibits Their Tumor Accumulation by Downregulating CXCR3/CXCL10 Axis

Chanyu Yue, Shudan Shen, Jiehui Deng, et al.

Cancer Immunol Res 2015;3:864-870. Published OnlineFirst May 29, 2015.